

Light-Induced Resistance Effect Observed in Nano Au Films Covered Two-Dimensional Colloidal Crystals

Shuai Liu,^{†,‡} Meizhen Huang,[†] Yanjie Yao,[†] Hui Wang,^{*,†} Kui-juan Jin,[‡] Peng Zhan,[§] and Zhenlin Wang[§]

[†]State Key Laboratory of Advanced Optical Communication Systems and Networks, Department of Physics and Astronomy, and Key Laboratory for Thin Film and Microfabrication Technology of the Ministry of Education, Research Institute of Micro/Nano Science and Technology, Shanghai Jiao Tong University, 800 Dongchuan Road, Shanghai 200240, China

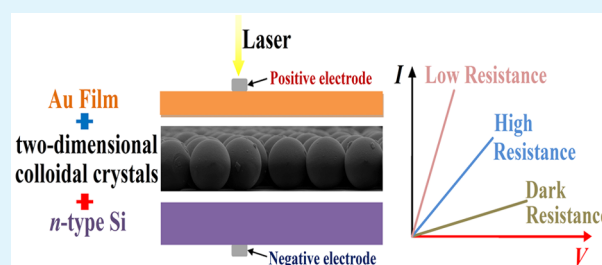
[#]North University of China, No. 3, Xueyuan Road, Taiyuan, ShanXi 030051, China

[‡]Collaborative Innovation Center of Quantum Matter, Institute of Physics, Chinese Academy of Sciences, Beijing 100190, China

[§]National Laboratory of Solid State Microstructures, Nanjing University, Nanjing 210093, China

ABSTRACT: Tailoring resistance response using periodic nanostructures is one of the key issues in the current research. Two-dimensional colloidal crystals (CCs) structure is one of popular periodic nanospheres' structures and most of reports are focused on anomalous transmission of light or biomedical applications. In this work, a light-induced resistance effect is observed on silicon-based Au films covered CCs, featuring a remarkable resistance change as much as 56% and resistance switching characteristic. The diffusion and recombination of photocarriers is the crucial factor for this effect. This finding will expand photoelectricity functionality and be useful for future development of CC-based photoelectric devices.

KEYWORDS: photoconductivity, colloidal crystals, metal-oxide-semiconductor, heterjunction, thin film devices and application



Effective manipulation of the resistance is an old and fascinating topic that has attracted tremendous interest because of its huge potential for various applications. Although extensive investigations have been reported on resistance effects, such as superconductivity effect,^{1,2} giant magneto-resistance effect,^{3,4} and electric-pulse-induced resistance switching effect,^{5,6} attempts for aiming to control the resistance are always sought in many disciplines, especially for versatile photoelectric materials. The structure of Au films covered two-dimensional colloidal crystals (CCs) is one of popular periodic nanospheres' materials, mainly investigated in a broad range of biological applications⁷ and anomalous transmission of light⁸ due to localized surface plasmon resonance⁹ (SPR). Different from that there are some reports on electrical characterization^{10–13} of other Au nanoparticles structures, to the best of our knowledge, the resistance property in this Au film covered CCs structure has never been reported before.

In this study, we will show a light-induced resistance effect observed on nano Au film covered two-dimensional CCs. Resistance behavior can be modulated in the CCs' structure with a fixed light position and applied voltage sweep is utilized to switch resistance states. This effect features the unipolar characteristic and a remarkable resistance change rate as much as 56% is achieved. The diffusion flow and recombination of photogenerated electron–hole pairs is the most crucial factor in this effect. As the prominent characteristic of this structure, localized SPR plays a relative assistance role. In the meanwhile, both the size of CCs and thickness of Au layer can also modulate the performance. Our finding reports the electrical

characterization of CCs system and makes this structure can be applied in photoelectrical areas, triggering further investigation of CC-based photoelectric devices.

The substrates used in the experiments are *n*-type Si (111). The thickness of the Si wafers is around 0.3 mm and the resistivity is within the range of 50–80 Ω cm at room temperature. The fabrication of the ordered metallic microstructures required sputtering a thin gold layer onto a monolayer of dielectric microspheres with an ion-beam coater (IBC Model 682, Gatan Corp.) to the desired thickness, at a rate of 1.2 \AA s^{-1} in a vacuum of 5×10^{-6} Torr. The thin gold film covering the microspheres consisted of a hexagonally close-packed array of gold half-shells, whose diameters can be controlled easily by choosing colloidal microspheres of different sizes. The microspheres are silica beads purchased from Duke Scientific Corps and the diameter is 1 μm . The two-dimensional CCs were prepared by injecting an aqueous solution of colloidal dispersion with a suitable concentration into a channel that was formed from two parallel quartz slides separated by a U-shaped spacer. The quartz slides had been pretreated to render their surface hydrophilic by soaking in a solution of 30% hydrogen peroxide at 80 $^{\circ}\text{C}$ for 30 min. After drying in air, CCs were grown within the channel under capillary force. Thus, the two-dimensional CCs were self-

Received: June 24, 2015

Accepted: August 24, 2015

Published: August 28, 2015

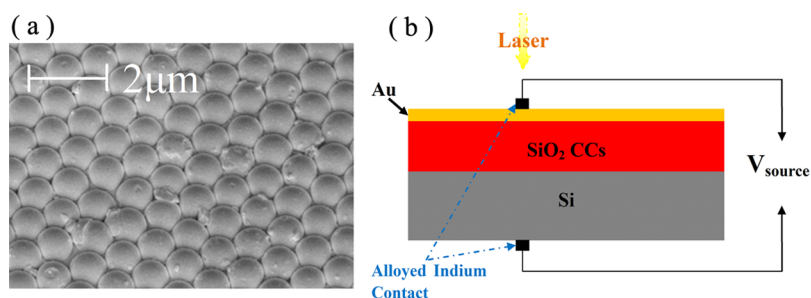


Figure 1. (a) Scanning electron microscopy (SEM) image of high ordered two-dimensional CCs. The microbeads are silica spheres and the diameter is 1 μm . (b) Measurement diagram of VI characteristics on Au/CCs/Si.

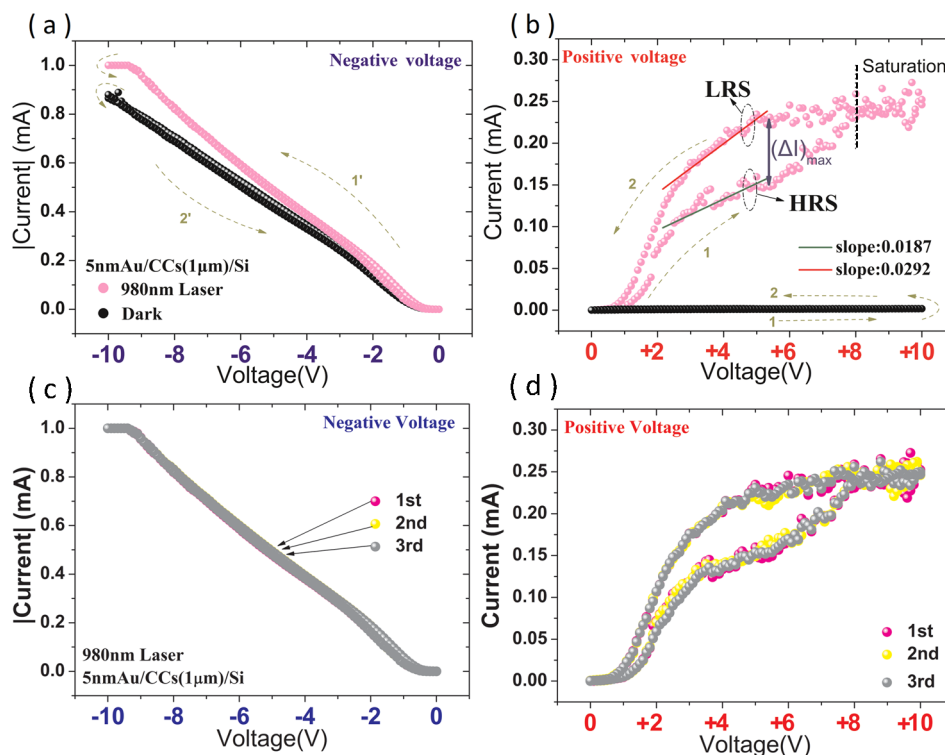


Figure 2. Current–voltage characteristics of a voltage sweeping mode measured on 5 nmAu/1 μm CCs/Si under (a) negative voltage and (b) positive voltage. Scanning steps are defined as step 1: 0–10 V, step 2: 10 V to \sim 0, step 1': 0 to approximately -10 V, step 2': -10 V to \sim 0. LRS and HRS represent low resistance state and high resistance states, respectively. (c, d) Three circles of current–voltage characteristics under negative voltage and positive voltage, respectively.

assembled onto the substrates using our previously reported method.^{7,8,14} The prepared CCs acted as a topographic pattern. Figure 1a shows the scanning electron microscopy (SEM) image of two-dimensional CCs. The microbeads are silica spheres and the diameter is 1 μm . The prepared silica spheres are densely packed and in touch with each other.

In this paper, all the samples are irradiated with 980 nm laser of a fixed 10 mW power, focusing by one convex lens (focal distance 10 cm) on a spot of ~ 50 μm in diameter at the ohmic contact on Au side without any spurious illumination (e.g., background light) reaching the samples, as shown in Figure 1b. The 980 nm laser is a semiconductor laser with a divergence angle of ~ 1 mrad. All the contacts (less than 1 mm in diameter) on the films are formed by alloying indium and show no measurable rectifying behavior, similar to our previous work.^{15–17} In our experiment, one ohmic contact is on the Au layer and the other ohmic contact is on the Si surface, with a voltage scan cycle using Keithley_4200.

According to Figure 2, it is clear that the resistance behavior in CCs' structure has unipolar modulation characteristic. The voltage is swept in a sequence of 0–positive–negative–0. In negative part, sweeping steps are defined as that step 1': 0 to -10 V and step 2': -10 V to 0. As shown in Figure 2a, current of dark condition is a little smaller than that of irradiated with 980 nm laser and there is no difference between step 1' and 2'. In positive part, step 1 and 2 are defined as 0 to 10 and 10 V to 0, respectively. Obviously, in Figure 2b, the current of the dark condition of step 1 is the same as that in step 2 and is much smaller than that irradiated with a 980 nm laser. It is interesting that there's an obvious current hysteresis phenomenon under illumination condition, showing a light-induced resistance effect. The positive voltage sweep can switch the structure from a high resistance state (HRS) in step 1 to a low resistance state (LRS) in step 2. In fact, in the case of illumination, the difference between LRS and HRS is very remarkable. The slope of curve is the value of conductance G (reciprocal of resistance

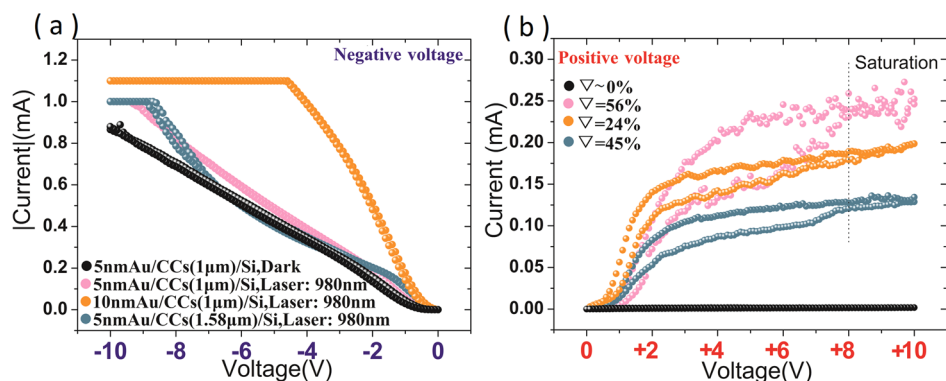


Figure 3. Current–voltage characteristics of a voltage sweeping mode with 980 nm laser measured on different structures under (a) negative voltage and (b) positive voltage.

R , $1S = 1 \Omega^{-1}$). G_{LRS} and G_{HRS} reach 2.92×10^{-2} mS and 1.87×10^{-2} mS, respectively. Corresponding error is 0.134×10^{-2} mS for G_{LRS} (4.6%) and 0.108×10^{-2} mS for G_{HRS} (5.8%). We can use ∇ to calculate resistance change rate easily, defined as eq 1. In Figure 2b, ∇ can reach up to 56% in the structure of Au(5 nm)/CCs(1 μ m)/Si with illumination, demonstrating that this effect has an obvious resistance change rate under the illumination between LRS and HRS. In contrast, there is no difference under dark condition or under negative voltage. The reason will be discussed later.

$$\nabla = \frac{G_{\text{LRS}} - G_{\text{HRS}}}{G_{\text{HRS}}} 100\% \quad (1)$$

In Figure 2b, we can obtain $(\Delta I)_{\text{max}}$ at the end of linear current region. Here $\Delta I = I_2 - I_1$, I_1 and I_2 are the current at the same voltage ($I_1 < I_2$). And $(\Delta I)_{\text{max}}$ marked in Figure 2b, is the maximum of ΔI . When the positive voltage increases, ΔI gets smaller and current is saturated, so we cannot distinguish between LRS and HRS. Our sample shows a typical saturation current characteristic in the heterojunction, known as inverse saturation current in PN junction. What's more, as light is blocked off, the current restores to the initial state without illumination. The light cannot destroy or change the structure to weaken the effect. This effect is nondestructive and sensitive for photon-generated carriers, which is totally different from other typical resistance effect caused by conduction electrons. It is a light-induced phenomenon.

To gain additional insights into this effect, we also investigated the stability and structure-dependence. As shown in Figure 2c, d, we measure three circles of current–voltage characteristics in the structure of Au(5 nm)/CCs(1 μ m)/Si with 980 nm laser illumination. It can be easily found that this light-induced effect has no obvious change after three circles, showing a remarkable stability. According to Figure 3a, under negative voltage, there is still no difference between voltage scanning step 1' and 2'. In Figure 3b, it can be clearly found that this effect also has a great bearing on both thickness of metal and diameter of CCs. For 5 nmAu/CCs(1.58 μ m)/Si, ∇ decreases to 45%; and ∇ is only 24% in the case of 10 nmAu/CCs(1 μ m)/Si. And all of these structures have a saturation current characteristic. And the plateau in Figure 3a comes from the current limitation: 1.1 mA for Au(10 nm)/CCs/Si and 1.0 mA for other structures.

When a beam of photons impinges on the sample, photons with energy higher than the silicon bandwidth can produce electron–hole pairs in the silicon at the illuminated area. Some

excited electrons will form the photocurrent, the other excited electrons will return to silicon to recombine with holes, as shown in Figure 4c. Meanwhile, localized SPR, the prominent characteristic of this structure, is collective electron charge oscillations in metallic nanoparticles that are excited by light. The electron oscillations can hold back the recombination of excited electrons with holes, leading to a larger photocurrent.

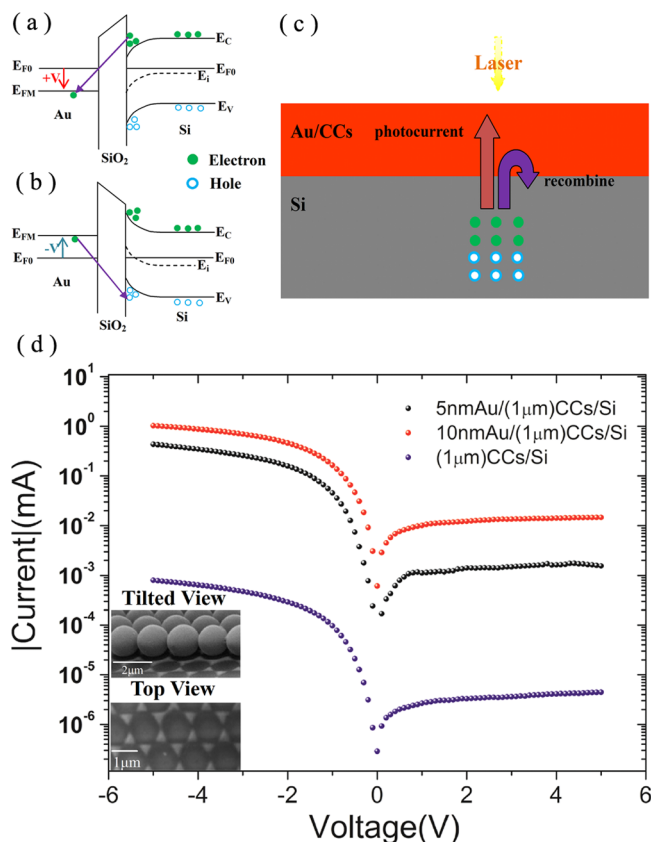


Figure 4. (a) Diagram of energy bands of Au/SiO₂/Si under positive voltage. (b) Diagram of energy bands of Au/SiO₂/Si under negative voltage. (c) Schematic diagram of photocarriers diffusion and recombination. (d) VI characteristics under dark condition of 1 μ m CCs for different Au films (0, 5, 10 nm). Inset: tilted view SEM consisted of two-dimensional CCs array and a gold triangular nanoparticle array; top view SEM of Au particles between adjacent CCs by removing the CCs after gold deposition.

That is why localized SPR can increase the current and play an assistance role in this effect.

For our samples, the structure of Au/CCs/Si is very important in this light-induced effect and provides explanation for why photocarriers can transit through CCs to change current behavior. Besides the wavy Au film of the surface, Au nanoparticles also make a gold triangular nanoparticle array between CCs and Si substrate, as shown in the inset SEM of Figure 4d. This part of Au particles increases the conductive ability. We measure the VI characteristics of our samples under dark condition (One electrode is on the Au film and the other is on the silicon). We find that current increases about 1000 times with Au deposited than without Au deposited and different Au film thickness also causes obvious current difference, as shown in Figure 4d. Because the wavy Au film just acts as electrode and does not affect VI characteristics, the difference of VI characteristics originates from the Au triangular nanoparticle array. Thus, with the help of Au triangular nanoparticles, electrons or photocarriers can tunnel through the SiO₂ CCs layer.

With an external voltage applied, the energy bands of the Si near the interface will bend. Figure 4a, b show simplified energy bands for different polarity voltage. With positive voltage (+V) applied, the Fermi level of the Au (E_{FM}) will drop, increasing the energy gap between conduction band of silicon (E_{C}) and E_{FM} . In this case, these excited electrons can easily tunnel to the Au surface due to a larger energy gap, resulting in amplification of current, consistent with Figure 2b. However, if the voltage is negative ($-V$), E_{FM} will rise, decreasing the energy gap between E_{C} and E_{FM} . Thus, excited electrons will recombine with holes more easily under negative voltage. So, we find that the current is significantly promoted by the laser within the positive voltage.

As for why there are two resistance states under the same positive voltage, it can be described as follows. During the fabrication process of CCs, abundant oxygen vacancies will be produced in the microstructure inevitably. When an external positive voltage is applied, it is easy to organize the oxygen vacancies in the oxide layer of the structure to be aligned along the two ohmic contacts direction, resulting from the oxygen migration to the anode. Thus, it forms the migration of oxygen vacancies based conduction filaments. The existence of conduction filament has been identified in the oxide layer of many materials and widely accepted as the origin of resistance change when voltage is applied on the structures.^{18–20} When the voltage increases, conductive filaments are built inside the CCs and act as electron transfer channels. With a 980 nm laser irradiation on the sample, the photoexcited electrons can transit to the surface through conductive filaments and constitute to the current. The current gets larger because of more conductive filaments. Even the applied voltage is the same, conductive filaments in voltage scanning step 2 are more than step 1, because the initial voltage of step 2 is the maximum and facilitates building more conductive filaments. That is the reason why there are different resistance states. And re-establishment of the conductive filament is needed again when applied voltage drops back to 0. This feature ensures that the materials can be reused. For dark condition, conduction electrons are much less than photoexcited electrons, showing a very small current in Figure 2b. Although the number of conductive filaments is still different under the same positive voltage, conduction electrons cannot effectively show the

difference between step 1 and 2, leading to there being no obvious phenomenon under dark conditions.

And the reason we did not observe the effect under negative voltage is determined by the feature of heterojunction. Under negative voltage, as majority carriers in metal of this heterojunction, the electrons tunnel reversely to the silicon, constituting a large current. Thus, the amount of photoexcited carriers and formed filaments is negligible comparing to this large current, leading to little change in current. On the contrary, photoexcited electrons will tunnel to the metal as positive voltage is applied, constituting a small current. So, filaments are non-negligible and can significantly enhance the current to form different resistance states.

In conclusion, a light-induced resistance effect dominated by photocarriers with a remarkable resistance change rate as much as 56% is achieved in the Au films covered two-dimensional CCs. This result is a complement of CCs' properties and adds the photoelectricity functionality to the CCs' system. This effect can stimulate both theoretical and experimental efforts in these two-dimensional ordered metallo-dielectric microstructures, especially to exploit their potential electrical or photoelectrical applications, such as optoelectronic switches, light memory device, light-controlled resistance circuit components.

AUTHOR INFORMATION

Corresponding Author

*E-mail: huiwang@sjtu.edu.cn.

Notes

The authors declare no competing financial interest.

ACKNOWLEDGMENTS

We acknowledge the financial support of the National Natural Science Foundation of China under Grants 11374214, 51271092, 61178083, and 51235008.

REFERENCES

- (1) Struzhkin, V. V.; Eremets, M. I.; Gan, W.; Mao, H. K.; Hemley, R. J. Superconductivity in Dense Lithium. *Science* **2002**, *298*, 1213–1215.
- (2) Onufrieva, F.; Pfeuty, P. Superconducting Pairing through the Spin Resonance Mode in High-temperature Cuprate Superconductors. *Phys. Rev. Lett.* **2009**, *102*, 207003.
- (3) Rao, C. N. R.; Cheetham, A. K. Giant Magnetoresistance in Transition Metal Oxides. *Science* **1996**, *272*, 369–370.
- (4) Muñoz-Rojas, F.; Fernández-Rossier, J.; Palacios, J. J. Giant Magnetoresistance in Ultrasmall Graphene Based Devices. *Phys. Rev. Lett.* **2009**, *102*, 136810.
- (5) Liu, S. Q.; Wu, N. J.; Ignatiev, A. Electric-pulse-induced Reversible Resistance Change Effect in Magnetoresistive Films. *Appl. Phys. Lett.* **2000**, *76*, 2749.
- (6) Waser, R.; Aono, M. Nanoionics-based Resistive Switching Memories. *Nat. Mater.* **2007**, *6*, 833–840.
- (7) Boisselier, E.; Astruc, D. Gold Nanoparticles in Nanomedicine: Preparations, Imaging, Diagnostics, Therapies and Toxicity. *Chem. Soc. Rev.* **2009**, *38*, 1759–1782.
- (8) Zhan, P.; Wang, Z. L.; Dong, H.; Sun, J.; Wu, J.; Wang, H. T.; Zhu, S. N.; Ming, N. B.; Zi, J. The Anomalous Infrared Transmission of Gold Films on Two-Dimensional Colloidal Crystals. *Adv. Mater.* **2006**, *18*, 1612–1616.
- (9) Li, Y. Y.; Pan, J.; Zhan, P.; Zhu, S. N.; Ming, N. B.; Wang, Z. L.; Han, W. D.; Jiang, X. Y.; Zi, J. Surface Plasmon Coupling Enhanced Dielectric Environment Sensitivity in a Quasi-three-dimensional Metallic Nanohole Array. *Opt. Express* **2010**, *18*, 3546–3555.
- (10) Joanis, P.; Tie, M.; Dhirani, A. A. Influence of Low Energy Barrier Contact Resistance in Charge Transport Measurements of

Gold Nanoparticle+Dithiol-Based Self-Assembled Films. *Langmuir* **2013**, *29*, 1264–1272.

(11) Wongsang, C.; Singjai, P. Resistance in Single-walled Carbon Nanotube Networks Formed on Gold Nanoparticle Templates. *J. Phys. D: Appl. Phys.* **2013**, *46*, 245106.

(12) Chen, S.; Yang, Y. Magnetochemistry of Gold Nanoparticle Quantized Capacitance Charging. *J. Am. Chem. Soc.* **2002**, *124*, 5280–5281.

(13) Lassesson, A.; Brown, S. A.; van Lith, J.; Schulze, M. Electrical Characterization of Gold Island Films: A Route to Control of Nanoparticle Deposition. *Appl. Phys. Lett.* **2008**, *93*, 203111.

(14) Love, J. C.; Gate, B. D.; Wolfe, D. B.; Paul, K. E.; Whitesides, G. M. Fabrication and Wetting Properties of Metallic Half-shells with Submicron Diameters. *Nano Lett.* **2002**, *2*, 891–894.

(15) Liu, S.; Wang, H.; Yao, Y. J.; Chen, L.; Wang, Z. L. Lateral Photovoltaic Effect Observed in Nano Au Film Covered Two-dimensional Colloidal Crystals. *Appl. Phys. Lett.* **2014**, *104*, 111110.

(16) Yu, C. Q.; Wang, H. Light-induced Bipolar-resistance Effect Based on Metal-oxide- semiconductor Structures of Ti/SiO₂/Si. *Adv. Mater.* **2010**, *22*, 966–970.

(17) Xiao, S. Q.; Wang, H.; Yu, C. Q.; Xia, Y. X.; Lu, J. J.; Jin, Q. Y.; Wang, Z. H. A Novel Position-sensitive Detector Based on Metal-oxide-semiconductor Structures of Co-SiO₂-Si. *New J. Phys.* **2008**, *10*, 033018.

(18) Chen, G.; Song, C.; Chen, C.; Gao, S.; Zeng, F.; Pan, F. Resistive Switching and Magnetic Modulation in Cobalt-Doped ZnO. *Adv. Mater.* **2012**, *24*, 3515–3520.

(19) Kim, D. C.; Seo, S.; Ahn, S. E.; Suh, D. S.; Lee, M. J.; Park, B. H.; Yoo, I. K.; Baek, I. G.; Kim, H. J.; Yim, E. K.; Lee, J. E.; Park, S. O.; Kim, H. S.; Chung, U. In.; Moon, J. T.; Ryu, B. I. Electrical Observations of Filamentary Conductions for the Resistive Memory Switching in NiO Films. *Appl. Phys. Lett.* **2006**, *88*, 202102.

(20) Choi, B. J.; Jeong, D. S.; Kim, S. K.; Rohde, C.; Choi, S.; Oh, J. H.; Kim, H. J.; Hwang, C. S.; Szot, K.; Waser, R.; Reichenberg, B.; Tiedke, S. Resistive Switching Mechanism of TiO₂ Thin Films Grown by Atomic-layer Deposition. *J. Appl. Phys.* **2005**, *98*, 033715.